INFLUENCE OF AL CONTENT ON MORPHOLOGY AND PROPERTIES OF PRIMARY $(Ti,Nb)_2AlC$ PARTICLES IN CAST Ti-Al-Nb-Mo MATRIX IN-SITU COMPOSITES

Alena KLIMOVÁ, Juraj LAPIN

Institute of Materials and Machine Mechanics, Slovak Academy of Sciences, Bratislava, Slovak Republic, EU, alena.klimova@savba.sk

https://doi.org/10.37904/metal.2019.749

Abstract

The effect of Al content on morphology, chemical composition, nanohardness and elastic modulus of primary $(Ti,Nb)_2AlC$ particles was investigated in in-situ composites with nominal composition Ti-xAl-8Nb-1Mo-0.1B-3.7C (at%), where x ranged from 38 to 45 at%. The in-situ composites were prepared by vacuum induction melting in the graphite crucibles and consecutive tilt casting into a graphite mould. Microstructural analyses show that the microstructure of the composites consists of irregular shaped, plate-like and regular shaped primary carbide particles which are relatively homogeneously distributed in the multiphase intermetallic matrix. The particles consist of $(Ti,Nb)_2AlC$ phase with small amount of (Ti,Nb)C phase in the cores of some coarse irregular shaped ones. The Al content has no effect on the measured volume fraction of the particles, but affects their morphology. The shape factor of the particles increases with increasing Al content. The size of the coarse irregular shaped particles decreases with increasing Al content. The solubility of Nb in $(Ti,Nb)_2AlC$ phase is not affected by the Al content and reaches only (0.78 ± 0.06) of the average Nb content in the composites. Mo dissolves predominantly in the matrix. The variation of the Al content in the composites has no significant effect on nanohardness and elastic modulus of $(Ti,Nb)_2AlC$ particles.

Keywords: Intermetallics, composites, casting, carbides, microstructure, hardness

1. INTRODUCTION

TiAl-based alloys belong to the progressive lightweight materials with a unique set of physical and mechanical properties for high temperature applications in automotive and aircraft industries [1]. However, two basic deficiencies of these alloys - poor ductility at room temperature and insufficient strength at high temperatures limit their wide-scale applications [2]. Due to a good combination of the properties of intermetallic matrix and reinforcement, in-situ intermetallic matrix composites reinforced with ceramic particles can overcome deficiencies of TiAl-based alloys at high temperatures. Among various ceramics used as the reinforcements, MAX phases (M is a transition metal, A is an A-group element and X is carbon), such as Ti_2AlC, show a significant contribution to toughening and reinforcing of TiAl-based matrix composites. The Ti_2AlC phase is characterized by a unique combination of both metallic and ceramic properties as high fracture resistance, excellent damage tolerance, good thermal and electrical conductivity, easy machinability, good thermal shock and oxidation resistance, high elastic modulus and thermochemical stability [3]. All these properties predetermine Ti_2AlC phase to be an excellent reinforcement of the intermetalic TiAl-based matrix in the form of coarse primary particles as well as fine secondary precipitates [4-11].

Several methods have been reported for processing of in-situ TiAl-based matrix composites reinforced with Ti_2AlC particles - powder metallurgy, mechanical alloying, reactive hot pressing, spark plasma sintering, vacuum induction melting and combustion synthesis [6,8]. Among them, induction melting and precise casting belong to a cost-effective way for production of complex shaped components [12,13], and thereby preparation of in-situ composites by this technique is also of large industrial interest.

The aim of this paper is to study the effect of Al content on the morphology and properties of primary $(Ti,Nb)_2AlC$ particles in Ti-xAl-8Nb-1Mo-0.1B-3.7C (at%) composites, where x = 38, 42 and 45 at%. The composites are prepared by vacuum induction melting in graphite crucibles followed by tilt casting. Chemical composition, size and morphology of primary $(Ti,Nb)_2AlC$ particles are investigated and their nanohardness and elastic modulus are measured.

2. EXPERIMENTAL PROCEDURE

The in-situ composites were prepared by vacuum induction melting in graphite crucibles with an inner diameter of 65 mm and length of 135 mm followed by tilt casting. The tilt casting was carried out into a cold graphite mould with an inner diameter of 38 mm and length of 230 mm. The as-cast cylindrical samples were cut transversally to smaller pieces with a diameter of 38 mm and length of 6 mm for metallographic observations using wire spark machining. Standard metallographic techniques and etching in a solution of 100 ml H_2O, 6 ml HNO_3 and 3 ml HF were used. Microstructure investigations were performed by optical microscopy (OM), scanning electron microscopy (SEM), scanning electron microscopy in back scattered electron mode (BSEM) and X-ray diffraction analysis (XRD). Chemical composition of the in-situ composites was analysed by energy-dispersive spectrometry (EDS) calibrated using the certified standards for measurements of the composition of carbides (TiC, Ti_2AlC). Average content of carbon in the samples was measured by LECO CS844 elemental analyser. Oxygen and nitrogen contents were analysed by a LECO ONH836 elemental analyser. Size, morphology and volume fraction of the coexisting phases were determined from the digitalised micrographs using computer image analyser and measured data were treated by statistical methods. Indentation nanohardness and elastic modulus measurements were carried out using ASMEC-Zwick/Roell nanoindenter with Berkovich tip of the indenter at an applied load of 0.01 N with the application of fast hardness and modulus measurement method.

3. RESULTS AND DISCUSSION

3.1. Chemical composition of the in-situ composites

The average chemical composition of the cast in-situ composites designated as 38Al, 42Al and 45Al is summarized in **Table 1**. The content of Al increases from 38.2 at% in the composite 38Al to 45.1 at% in the 45Al. The content of Nb, Mo and C in all three studied composites varies only within the experimental error of the measurements. It should be noted that the content of oxygen and nitrogen do not exceed 850 wt.ppm and 450 wt.ppm, respectively.

Table 1 Chemical composition of the in-situ composites (at%)

Composites	Element				
	Al	Ti	Nb	Mo	C
38Al	38.2 ± 0.3	49.1 ± 0.3	8.0 ± 0.1	1.0 ± 0.1	3.7 ± 0.1
42Al	42.1 ± 0.3	45.2 ± 0.4	8.1 ± 0.1	0.8 ± 0.1	3.8 ± 0.1
45Al	45.1 ± 0.1	42.6 ± 0.1	7.9 ± 0.1	0.7 ± 0.1	3.8 ± 0.1

3.2. Microstructure and phase analysis

The microstructure of the composites 38Al, 42Al and 45Al consists of primary carbide particles which are relatively homogeneously distributed in the multiphase intermetallic matrix (**Figure 1**). The XRD patterns shown in **Figure 2a** and EDS analysis (**Table 2**) indicate that the primary particles formed during solidification belong to hexagonal (*hP8*) type MAX-phase $(Ti,Nb)_2AlC$ (region 1). In the core of some coarse irregular $(Ti,Nb)_2AlC$ particles, small regions of (Ti,Nb)C are observed (region 2), as seen in **Figure 2b**. Both $(Ti,Nb)_2AlC$ and (Ti,Nb)C particles contain Nb. The solubility of Nb in $(Ti,Nb)_2AlC$ phase reaches only (0.78 ± 0.06) of the average Nb content measured in the composites and is not affected by the average Al content. The similar tendency of lower content of Nb in MAX phase particles was described also by Fang *et al*. [9], where the lower content of Nb in $(Ti,Nb)_2AlC$ was ascribed to the preferential segregation of Nb in the matrix. In all primary carbide particles including their cores, Mo content was under detectable limits of the applied EDS analysis.

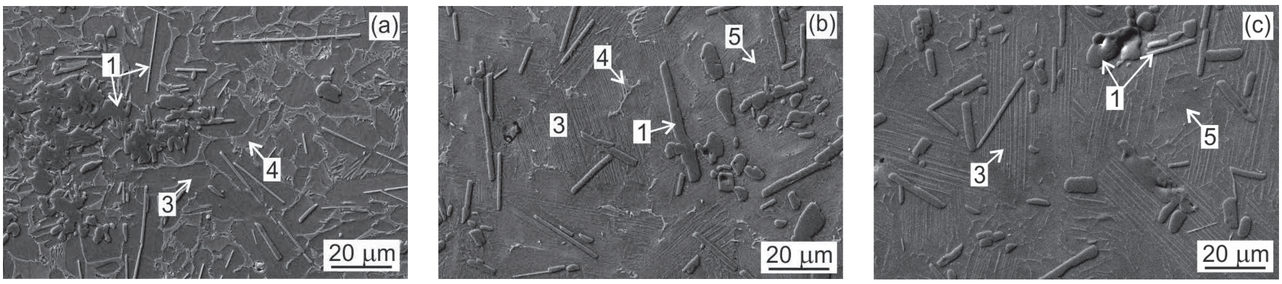

Figure 1 SEM micrographs showing the typical microstructure of the in-situ composites: (a) 38Al, (b) 42Al, (c) 45Al

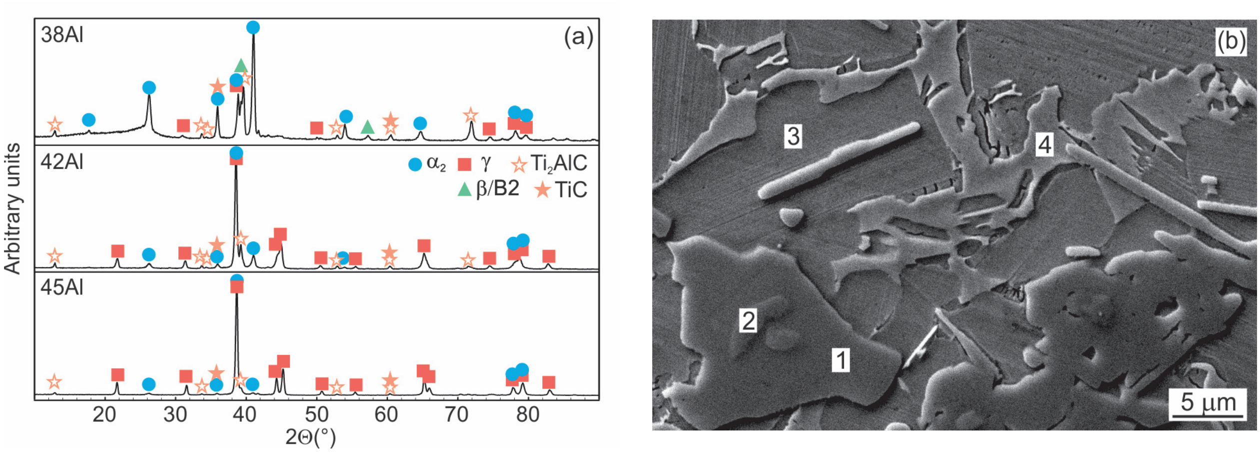

Figure 2 (a) XRD patterns of 38Al, 42Al and 45Al in-situ composites; (b) SEM micrograph showing microstructure of 38Al in-situ composite

The matrices of the studied in-situ composites are formed by $\alpha_2(Ti_3Al)$, γ(TiAl) and β/B2(Ti)-phase. The chemical compositions of the particular regions of the matrix designated as 3 to 5 in **Figure 1** and **Figure 2b** are summarized in **Table 2**. The β/B2-phase (region 4) is enriched by Nb and Mo. Both these elements act as strong β stabilizers while the β/B2 stabilizing effect of Mo is more pronounced than that of Nb [14].

Figure 3 shows volume fraction of coexisting regions and size of primary carbide particles of the studied composites. It is clear that the Al content has no effect on the measured volume fraction of the carbide particles (V_p), but significantly affects the volume fraction of other coexisting phases in the matrix, as seen in **Figure 3a**. The volume fraction of (Ti,Nb)C regions in the cores of some coarse particles is found to be not affected by the Al content and is measured to be (1.4 ± 0.2) vol%. The volume fraction of the β/B2-phase in the matrix decreases from 25 vol% in the composite 38Al to 1 vol% in the composite 45Al. Beside the lamellar α_2+γ colonies, larger γ single phase areas (region 5) are observed in the composites 42Al (**Figure 1b**) and 45Al (**Figure 1c**), what is connected with a change of solidification paths of the studied composites with the increasing Al content. According to existing Ti-Al-C phase diagrams [15], a cubic TiC_{1-x} phase exists in the studied alloys already at the melt temperature of about 1690 °C. During solidification, the TiC_{1-x} phase transforms to the hexagonal H-Ti_2AlC phase. Since no phase diagrams which describe phase transformations in the studied TiAl-based alloys with chemical composition close to 8 at% of Nb, 1 at% Mo and 3.6 at% of C exist, the solidification path of the studied in-situ composites can be estimated on the base of existing phase diagrams for Nb- [16-18], Nb-Mo- [19] and C-doped [15] alloys. Combination of β stabilizing elements as Nb and Mo [14] and α stabilizing C [20] certainly modifies both types of described Ti-Al systems. Based on the microstructural observations and existing phase diagrams, the primary (Ti,Nb)C particles present in the liquid (L) transforms to $(Ti,Nb)_2AlC$ and a new equilibrium L + $(Ti,Nb)_2AlC$ is created during solidification. These particles serve as nucleation sites of the β-phase. The stable microstructure formed during solid phase state transformations depends on the Al content and changes from H+α_2+γ+β/B2 in the composite 38Al to γ+H in 45Al.

Table 2 Chemical composition of the coexisting phases in the 38Al, 42Al and 45Al in-situ composites (at%)

Sample	Region	Phase composition	Element				
			Ti	Al	Nb	Mo	C
38Al	1	$(Ti,Nb)_2AlC$	41.9± 1.3	24.0 ± 0.6	5.8 ± 0.7	-	28.3 ± 1.0
	2	(Ti,Nb)C	42.0 ± 4.8	4.8 ± 3.1	4.8 ± 1.5	-	48.4 ± 2.0
	3	α_2+γ	49.8 ± 0.3	41.6 ± 0.2	7.9 ± 0.2	0.8 ± 0.1	-
	4	β/B2	51.9 ± 0.5	36.4 ± 0.4	9.6 ± 0.3	1.9 ± 0.4	-
42Al	1	$(Ti,Nb)_2AlC$	40.7 ± 1.4	23.9 ± 1.2	6.9 ± 0.6	-	28.4 ± 2.5
	2	(Ti,Nb)C	40.6 ± 1.1	2.8 ± 1.2	6.3 ± 0.1	-	50.3 ± 1.7
	3	α_2+γ	45.4 ± 0.2	45.0 ± 0.3	8.8 ± 0.2	0.8 ± 0.1	-
	4	β/B2	47.8 ± 1.2	38.0 ± 1.7	11.3 ± 0.4	2.9 ± 0.5	-
	5	γ	45.3 ± 0.4	45.2 ± 0.6	8.8 ± 0.4	0.8 ± 0.2	-
45Al	1	$(Ti,Nb)_2AlC$	41.2 ± 2.3	23.2 ± 1.8	6.7 ± 0.7	-	28.9 ± 1.3
	2	(Ti,Nb)C	40.4 ± 6.5	5.7 ± 3.2	5.1 ± 1.6	-	48.8 ± 2.7
	3	α_2+γ	43.5 ± 0.8	47.3 ± 1.1	8.4 ± 0.5	0.8 ± 0.1	-
	5	γ	42.5 ± 0.8	48.9 ± 1.2	7.8 ± 0.7	0.8 ± 0.1	-

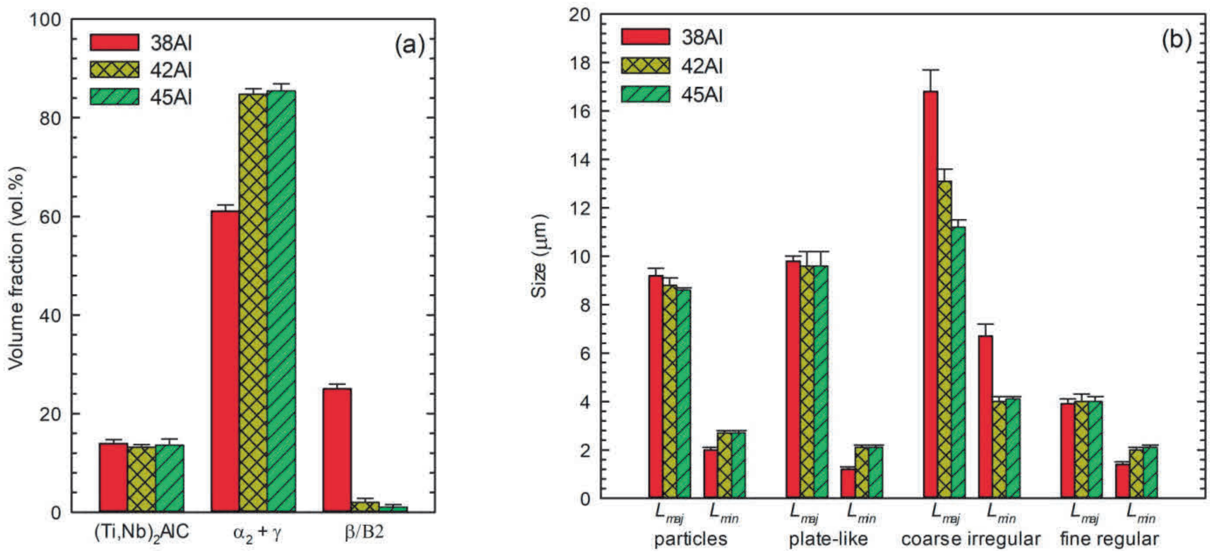

Figure 3 (a) Volume fraction of $(Ti,Nb)_2AlC$ particles, lamellar α_2+γ matrix and β/B2 regions; (b) Length of major axis L_{maj} and length of minor axis L_{min} of particles and separate groups of plate-like, coarse irregular and fine regular particles

Assuming a relationship for circularity in the form $F = (4\pi A/P^2)$, where A is the area and P is the perimeter, the shape factor F of the particles increases from 0.34 in the composite 38Al to 0.50 in the 45Al. Three types of morphologically different primary carbide particles are distinguished in the microstructure: (i) coarse irregular shaped carbides (75 % of measured volume fraction V_p), (ii) plate-like (20 % of V_p) and (iii) fine regular shaped particles (5 % of V_p). The Al content has a significant effect on the size and morphology of the primary particles, as shown in **Figure 3b**. The size of the coarse irregular shaped particles decreases with increasing Al content. Presence of higher volume fraction of β/B2-phase in the 38Al composite results in the formation of much coarser irregular shaped and thinner plate-like particles in comparison with those in the 42Al and 45Al composites. As shown by Lapin et al. [21], due to the limited plastic deformation of coarse $(Ti,Nb)_2AlC$ particles, cracks formed during compressive deformation preferentially initiate within the coarse irregular shaped particles and at the carbide particle/matrix interfaces. From this point of view, larger size of coarse particles in the 38Al composite makes this composite less resistant to the damage than that of the composites 42Al and 45Al with higher content of Al.

3.3. Hardness and elastic modulus

The variation of the Al content in the composites has no significant effect on nanohardness H_{IT} and elastic modulus E_{IT} of $(Ti,Nb)_2AlC$ particles, though the slight decrease of H_{IT} and E_{IT} with the increasing Al content was observed, as shown in the **Table 3**. Nanohardness and elastic modulus of (Ti,Nb)C phase regions in the core of some coarse particles was estimated to be (23.7 ± 0.8) GPa and (316 ± 8) GPa, respectively.

Table 3 Nanohardness and elastic modulus of $(Ti,Nb)_2AlC$ phase in particles

Composite	H_{IT} (GPa)	E_{IT} (GPa)
38Al	10.7 ± 0.7	216 ± 8
42Al	10.4 ± 0.4	210 ± 7
45Al	9.9 ± 0.5	204 ± 5

4. CONCLUSION

The increasing content of Al in the studied in-situ composites has no effect on the measured volume fraction of the reinforcing primary $(Ti,Nb)_2AlC$ particles, but affects their morphology. The shape factor of the particles increases with increasing Al content. The size of the coarse irregular shaped particles decreases with increasing Al content. The solubility of Nb in $(Ti,Nb)_2AlC$ phase is not affected by the Al content and reaches only (0.78 ± 0.06) of the average Nb content in the composites. Mo dissolves predominantly in the matrix. The variation of the Al content in the composites has no significant effect on nanohardness and elastic modulus of $(Ti,Nb)_2AlC$ particles.

ACKNOWLEDGEMENTS

This work was financially supported by the Slovak Research and Development Agency under the contract APVV-15-0660. The authors would like to thank to Dr. P. Oslanec, Jr. and Dr. T. Švantner for measurements of carbon content by LECO CS844 elemental analyser.

REFERENCES

[1] KIM, Y.-W. and KIM, S.-L. Advances in Gammalloy Materials - Processes - Application Technology: Successes, Dilemmas, and Future. *The Journal of The Minerals, Metals & Materials Society (TMS)*. 2018. vol. 70, pp. 553-560. doi:10.1007/s11837-018-2747-x.

[2] APPEL, F., CLEMENS, H. and FISCHER, F.D. Modeling concepts for intermetallic titanium aluminides. *Progress in Materials Science*. 2016. vol. 81, pp. 55-124. doi:10.1016/j.pmatsci.2016.01.001.

[3] BARSOUM, M.W. and RADOVIC, M. Elastic and mechanical properties of the MAX phases. *Annual Review of Materials Research*. 2011. vol. 41, pp.195-227. doi:10.1146/annurev-matsci-062910-100448.

[4] LAPIN, J., KLIMOVÁ, A., GABALCOVÁ, Z., PELACHOVÁ, T., BAJANA, O. and ŠTAMBORSKÁ, M. Microstructure and mechanical properties of cast in-situ TiAl matrix composites reinforced with $(Ti,Nb)_2AlC$ particles. *Materials and Design*. 2017. vol. 133, pp. 404-415. doi:10.1016/j.matdes.2017.08.012.

[5] ŠTAMBORSKÁ, M., LAPIN, J. and BAJANA, O. Effect of carbon on room temperature compressive behaviour of Ti-44.5Al-8Nb-0.8Mo-xC alloys prepared by vacuum induction melting. *Kovove Materialy*. 2018. vol. 56, pp. 349-356.

[6] SONG, X.J., CUI, H.Z., HOU, N., WEI, N., HAN, Y., TIAN, J. and SONG, Q., Lamellar structure and effect of Ti_2AlC on properties of prepared in-situ TiAl matrix composites. *Ceramics International*. 2016. vol. 42, pp. 13586-13592.

[7] SONG, X., CUI, H., HAN, Y., HOU, N., WEI, N., DING, L. and SONG, Q. Effect of carbon reactant on microstructures and mechanical properties of $TiAl/Ti_2AlC$ composites. *Materials Science and Engineering A*. 2017. vol. 684, pp. 406-412. doi:10.1016/j.msea.2016.12.069.

[8] CHEN, R., FANG, H., CHEN, X., SU, Y., DING, H., GUO, J. and FU, H. Formation of TiC/Ti_2AlC and $\alpha_2+\gamma$ in *in-situ* TiAl composites with different solidification paths. *Intermetallics*. 2017. vol. 81, pp. 9-15.

[9] FANG, H., CHEN, R., GONG, X., SU, Y., DING, H., GUO, J. and FU, H. Effects of Nb on microstructure and mechanical properties of Ti42Al2.6C alloys. *Advanced Engineering Materials*. 2018. vol. 20, art. no. 1701112, pp. 1-9. doi:10.1002/adem.201701112.

[10] CEGAN, T. and SZURMAN, I., Thermal stability and precipitation strengthening of fully lamellar Ti-45Al-5Nb-0.2B-0.75C alloy. *Kovove Materialy*. 2018. vol. 55, pp. 421-430. doi:10.4149/km_2017_6_421.

[11] KLIMOVA, A. and LAPIN, J. Effects of C and N additions on primary MAX phase particles in intermetallic Ti-Al-Nb-Mo matrix in-situ composites prepared by vacuum induction melting. *Kovove Materialy*. 2019. vol. 57, pp. 151-157. doi: 10.4149/km_2019_3_151

[12] BÜNCK, M., STOYANOV, T., SCHIEVENBUSCH, J., MICHELS, H. and GUSSFELD, A. Titanium aluminide casting technology development. *The Journal of The Minerals, Metals & Materials Society (TMS)*. 2017. vol. 69, pp. 2565--2570. doi:10.1007/s11837-017-2534-0.

[13] GÜTHER, V., ALLEN, M., KLOSE, J. and CLEMENS, H. Metallurgical processing of titanium aluminides on industrial scale. *Intermetallics*. 2018. vol 103, pp. 12-22. doi:10.1016/j.intermet.2018.09.006.

[14] KAINUMA, R., FUJITA, Y., MITSUI, H., OHNUMA, I. and ISHIDA, K. Phase equilibria among α (hcp), β (bcc) and γ ($L1_0$) phases in Ti-Al base ternary alloys. *Intermetallics*. 2000. vol. 8, pp. 855-867

[15] WITUSIEWICZ, V.T., HALLSTEDT, B., BONDAR, A.A., HECHT, U., SLEPTSOV, S.V. and VELIKANOVA, T.Y. Thermodynamic description of the Al-C-Ti system. *Journal of Alloys and Compounds*. 2015. vol. 623, pp. 480-496. doi:10.1016/j.jallcom.2014.10.119.

[16] CHLADIL, H.F., CLEMENS, H., LEITNER, H., BARTELS, A., GERLING, R., SCHIMANSKY, F.P. and KREMMER, S. Phase transformations in high niobium and carbon containing γ-TiAl based alloys. *Intermetallics*. 2006. vol. 14, pp. 1194-1198. doi:10.1016/j.intermet.2005.11.016.

[17] CHEN, G.L., XU, X.J., TENG, Z.K., WANG, Y.L. and LIN, J.P. Microsegregation in high Nb containing TiAl alloy ingots beyond laboratory scale. *Intermetallics*. 2007. vol. 15, pp. 625-631. doi:10.1016/j.intermet.2006.10.003.

[18] BONDAR, A.A., WITUSIEWICZ, V.T., HECHT, U., REMEZ, M.V, VOBLIKOV, V.M., TSYGANENKO, N.I., YEVICH, Ya.I., PODREZOV, Yu.M. and VELIKANOVA, T.Ya. Structure and properties of titanium - aluminum alloys doped with niobium and tantalum. *Powder Metallurgy and Metal Ceramics*. 2011. vol. 50, pp. 397-415.

[19] SCHWAIGHOFER, E., CLEMENS, H., MAYER, S., LINDEMANN, J., KLOSE, J., SMARSLY, W. and GÜTHER, V. Microstructural design and mechanical properties of a cast and heat-treated intermetallic multi-phase γ-TiAl based alloy. *Intermetallics*. 2014. vol. 44 , pp. 128-140. doi:10.1016/j.intermet.2013.09.010.

[20] PERDRIX, F., TRICHET, M.F., BONNENTIEN, J.L., CORNET, M. and BIGOT, J. Relationships between interstitial content, microstructure and mechanical properties in fully lamellar Ti-48Al alloys, with special reference to carbon, *Intermetallics*. 2001. vol. 9, pp. 807-815. doi:10.1016/S0966-9795(01)00066-8.

[21] LAPIN, J., ŠTAMBORSKÁ, M., KAMYSHNYKOVA, K., PELACHOVÁ, T., KLIMOVÁ, A. and BAJANA, O. Room temperature mechanical behaviour of cast *in-situ* TiAl matrix composite reinforced with carbide particles. *Intermetallics*. 2019. vol. 67, pp. 158-165. doi:10.1016/j.intermet.2018.11.007.